

List of Figures

7.1	<i>The global MOC as computed from a Coupled General Circulation Model (CGCM). We clearly see the presence of the North Atlantic Deep Water cell, the interhemispheric meridional circulation, a locally-circulating deacon Cell, and two SubTropical Cells. Each meridional cell is driven by different dynamics and all together set up the global ocean circulation.</i>	6
7.2	<i>Schematic of a single-celled meridional overturning circulation. Sinking is concentrated at high latitude and upwelling spread out over lower latitudes. [from Vallis (2006)]</i>	8
7.3	<i>Wind forcing in the subtropics pushes the warm surface water into the fluid interior, deepening the thermocline as well as circulating as a gyre. [from Vallis (2006)]</i>	9
7.4	<i>Scaling of the thermocline. The diagonal lines mark the diffusive thermocline of thickness δ and depth $D(y)$. [from Vallis (2006)] .</i>	13
7.5	<i>The role of vertical (diapycnal) diffusion in the MOC, replacing a deep tropical warm source with diapycnal diffusion that reaches below the effect of high latitude cooling. [from Talley et al. (2011)]</i>	14
7.6	<i>Stommel-Arons ocean model of the abyssal circulation. Convection at high latitudes provides a localized mass-source to the lower layer, and upwelling through the thermocline provides a more uniform mass sink. [from Vallis (2006)]</i>	15
7.7	<i>Abyssal circulation in a spherical sector and in a corresponding Cartesian rectangle. [from Vallis (2006)]</i>	17
7.8	<i>Mass budget in an idealized abyssal ocean. Polewards of some latitude y, the mass source (S_0) plus the poleward mass flux across y (T_I) are equal to the sum of the equatorward mass flux in the western boundary current (T_W) and the integrated loss due to upwelling (U) polewards of y. [from Vallis (2006)]</i>	18

7.9	<i>Schematic of a Stommel–Arons circulation in a single sector. The transport of the western boundary current is greater than that provided by the source at the apex, illustrating the property of recirculation. The transport in the western boundary current T_W decreases in intensity equatorwards, as it loses mass to the polewards interior flow, and thence to upwelling. The integrated sink, due to upwelling, U, exactly matches the strength of the source, S_0. [from Vallis (2006)]</i>	20
7.10	<i>(a) Abyssal circulation model. After Stommel and Arons (1960a). (b) Laboratory experiment results looking down from the top on a tank rotating counterclockwise around the apex (S_0) with a bottom that slopes towards the apex. There is a point source of water at S_0. The dye release in subsequent photos shows the Deep Western Boundary Current, and flow in the interior S_I beginning to fill in and move towards S_0. [from Talley et al. (2011)]</i>	21
7.11	<i>Global abyssal circulation model, assuming two deep water sources (filled circles near Greenland and Antarctica). [from Talley et al. (2011)]</i>	22
7.12	<i>One feature of the solution is a deep western boundary current that flows southward in the Atlantic Ocean. This is consistent with observations. For example, high oxygen water is formed in the North Atlantic and flows southward in the deep western boundary current. [from the WOCE Atlas]</i>	23
7.13	<i>Time series of different components of volume transports from the RAPID Array (2004-2019).</i>	24
7.14	<i>Time mean (2004-2019) of the overturning stream function at 26.5N from RAPID.</i>	25

Contents

7	Overturing Circulations	5
7.1	Depth of the wind's influence and the main thermocline . . .	7
7.1.1	Munk's hypotesis	7
7.1.2	Scaling and dynamics of the main thermocline	9
7.2	A model for the oceanic abyssal flow:	
	The Stommel-Arons model	14
7.2.1	A sector ocean	17
7.3	Wind-driven Overturing	24

Overturning Circulations

The Meridional Overturning Circulation, or MOC, of the ocean is the circulation associated with sinking mostly at high latitudes and upwelling elsewhere, with the *meridional transport mostly taking place below the main thermocline*. The theory explaining the MOC is not nearly as settled as that of the quasi-horizontal wind-driven circulation, but considerable progress has been made, in particular with a significant re-thinking of the fundamentals, especially concerning the role of the wind in maintaining a deep MOC.

That there is a deep circulation has been known for a long time, largely from observations of tracers such as temperature, salinity, and constituents such as dissolved oxygen and silica. We can also take advantage of numerical models that are able to assimilate observations (mainly from hydrographic measurements, floats and satellites) and produce a state estimate of the overturning circulation that is consistent with both the observations and the equations of motion (see Fig.7.1). We see that the water does not all upwell in the subtropics as we assumed so far in the simple thermocline scalings.

In fact, much of the mid-depth circulation more-or-less follows the isopycnals that span the two hemispheres, sinking in the North Atlantic and upwelling in the Southern Ocean, with the transport in between being, at least in part, adiabatic (see Fig.7.1).

The MOC used to be known as the ‘thermohaline’ circulation, reflecting the belief that it was primarily driven by buoyancy forcing arising from gradients in temperature and salinity. Such a circulation requires that the diapycnal mixing must be sufficiently large, but many measurements have suggested this is not the case and that has led to a more recent view that the MOC is at least partially, and perhaps primarily, mechan-

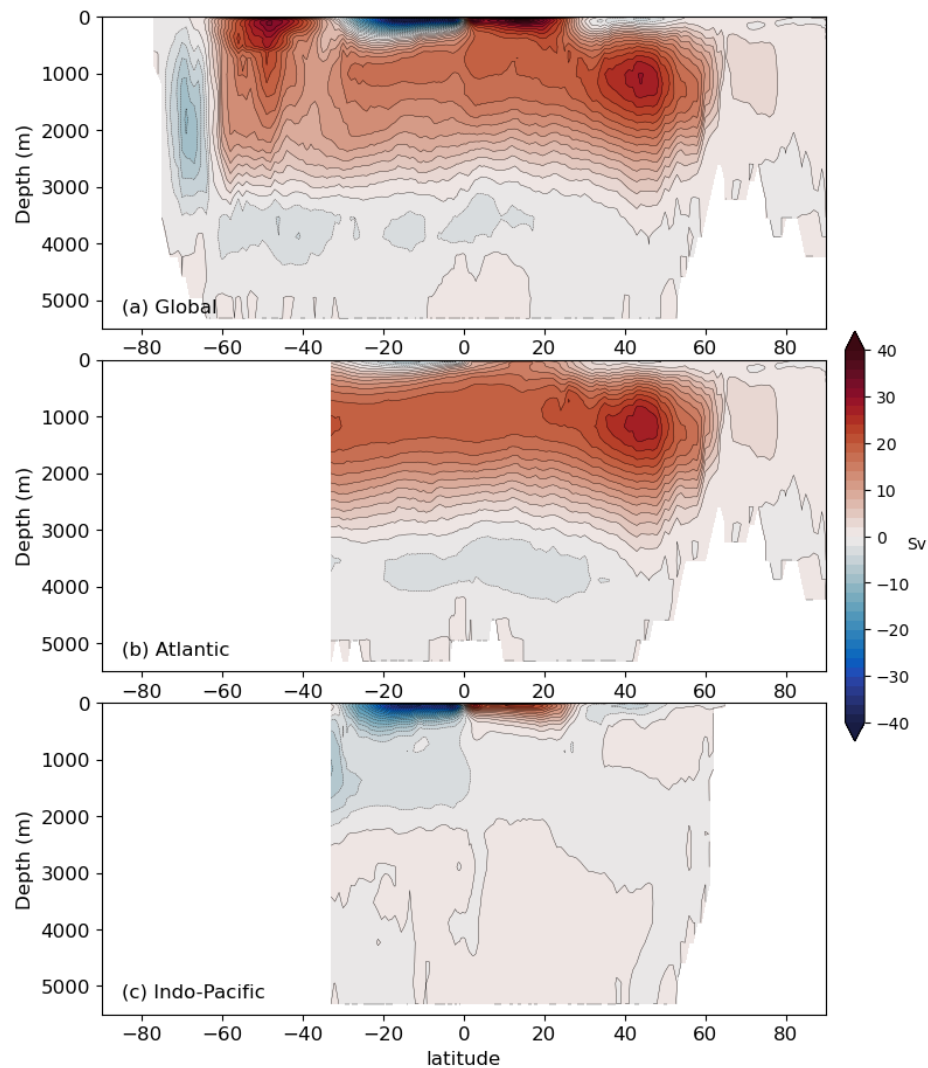


Figure 7.1: The global MOC as computed from a Coupled General Circulation Model (CGCM). We clearly see the presence of the North Atlantic Deep Water cell, the interhemispheric meridional circulation, a locally-circulating deacon Cell, and two SubTropical Cells. Each meridional cell is driven by different dynamics and all together set up the global ocean circulation.

ically driven, mostly by winds, and so *along* isopycnals instead of *across* them. However, the situation is not wholly settled, and it is almost certain that both buoyancy and wind forcing, as well as diapycnal diffusion, play a role.

7.1 Depth of the wind's influence and the main thermocline

We now make a first step towards understanding what sets the depth at which reaches the influence of the wind-driven circulation. How deep is the wind's influence?

7.1.1 Munk's hypothesis

What is actually giving rise to the observed density structure of the upper ocean? in particular to the main thermocline (yes, there are more thermocline regimes ... but we will leave those for another day ...).

Supposing there is net surface warming at low latitudes and net cooling at high latitudes, this will maintain a meridional temperature gradient at the surface. We can thus presume that there will be water rising at the surface at low latitudes and then returning to polar regions where they sink. The dynamics of this meridional overturning circulation (MOC) will set a balance between upward motion and downward diffusion, responsible for the depth at which density (or in this case temperature) will change very rapidly in the vertical.

After cold water has sunk at high latitudes, this will create, through hydrostasy, a higher pressure in the deep ocean at high latitudes than at low latitudes, where the water is much warmer. *For this reason the bottom water will move equatorward and fill the abyss.* As this water moves it is warmed by heat diffusion from above (diffusion is directed downwards), keeping the circulation going. There is thus a vertical density(temperature) gradient throughout the basin but in the polar regions where cold water sinks.

Given the simple cartoon depicting the ocean, with polar waters upwelling into a region of warmer water, we can consider a simple advective-diffusive balance. Munk (1966) hypothesized that the below 1000 m the flow obeys the vertical advection-diffusion equation, i.e. we can neglect horizontal transports of temperature and salinity.

$$w \frac{\partial T}{\partial z} = K_v \frac{\partial^2 T}{\partial z^2} \quad (7.1)$$

where w is the vertical velocity, K_v an eddy vertical diffusivity and T the temperature. w is positive, towards the surface, and diffusion is directed downwards, producing a balance between the two circulations.

If w and K_v are constants, $T = T_T$ at $z = 0$ and $T = T_B$ at $z = -\infty$, we get

$$T = (T_T - T_B) e^{zw/K_v} + T_B. \quad (7.2)$$

The temperature falls exponentially away from the surface. The scale of the exponential decay is

$$\delta = \frac{K_v}{w}. \quad (7.3)$$

This is an estimate of the thickness of the thermocline. Munk fitted temperature and salinity data from the central Pacific with these functions to estimate K_v . The central Pacific is a good place because it has low horizontal velocities in the deep ocean. Munk obtained values of $K_v \sim 1.3 \times 10^{-4} \text{ m}^2 \text{ s}^{-1}$.

If we use $w = 10^{-7} \text{ m s}^{-1}$ and a range of diffusivity K_v between 10^{-4} and $10^{-5} \text{ m}^2 \text{ s}^{-1}$, we get an e-folding vertical scale between $\delta=100 \text{ m}$ and 1000 m . The first case is too shallow, but the second is closer to observations. According to Munk's recipe, the upwelling of deep waters is driven by downward diffusion of heat from the surface and the simple model predicts that the temperature gradient is concentrated in the upper ocean.

Cold water is upwelling and only needs to warm up as it approaches the warm upper surface. If K_v were very very small there would just be a

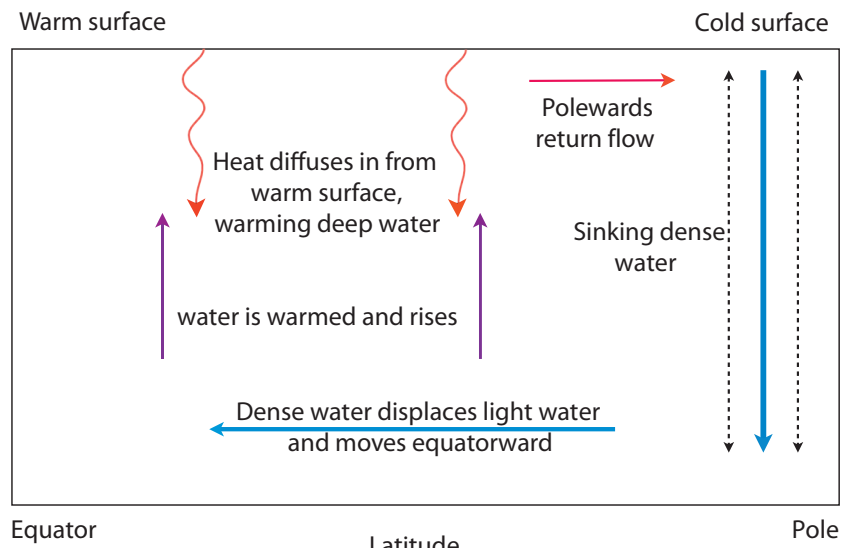


Figure 7.2: Schematic of a single-celled meridional overturning circulation. Sinking is concentrated at high latitude and upwelling spread out over lower latitudes. [from Vallis (2006)]

thin boundary layer at the top of the ocean, and the overturning circulation would be very weak because almost the entire ocean would be as dense as the cold polar surface waters.

7.1.2 Scaling and dynamics of the main thermocline

The flow, which has a small Rossby number and very large scale of motion, obeys the planetary-geostrophic equations

$$f \times \mathbf{u} = -\nabla\phi, \quad (7.4)$$

$$\frac{\partial\phi}{\partial z} = b, \quad (7.5)$$

$$\nabla \cdot \mathbf{v} = 0, \quad (7.6)$$

$$\frac{D b}{D t} = \kappa \frac{\partial^2 b}{\partial z^2}. \quad (7.7)$$

Which are the momentum equations, hydrostasy, continuity and the thermodynamics equations respectively. These equations hold for the interior

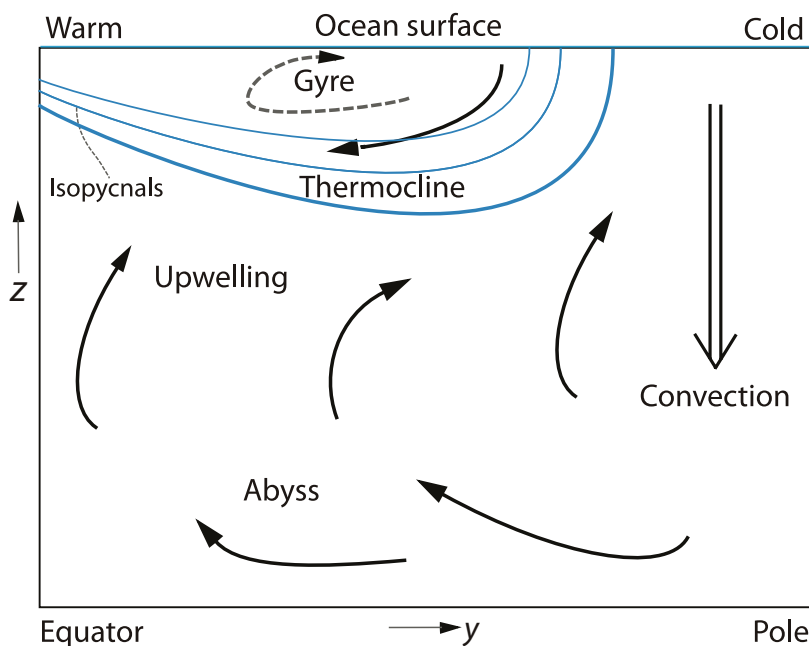


Figure 7.3: Wind forcing in the subtropics pushes the warm surface water into the fluid interior, deepening the thermocline as well as circulating as a gyre. [from Vallis (2006)]

flow, below the Ekman layer, and we insert the effects of the wind stress by specifying a vertical velocity W_E .

A diffusive scale

Suppose there is no wind forcing, and the only possible driver of the circulation is diffusivity: what would be the depth of the *diffusive thermocline* in the subtropical gyre?

We again use the approximation of an advective-diffusive balance. We take the curl of the momentum equations and use mass continuity to obtain the linear vorticity equation. We take the vertical derivative of the momentum equation and use hydrostasy to obtain the thermal wind:

$$w \frac{\partial b}{\partial z} = \kappa \frac{\partial^2 b}{\partial z^2}, \quad \beta v = f \frac{\partial w}{\partial z}, \quad f \frac{\partial \mathbf{u}}{\partial z} = \mathbf{k} \times \nabla b \quad (7.8)$$

and their scales are

$$\frac{W}{\delta} = \frac{\kappa}{\delta^2}, \quad \beta U = f \frac{W}{\delta}, \quad f \frac{U}{\delta} = \frac{\Delta b}{L} \quad (7.9)$$

The first scaling is the same as the first diffusive scaling (Munk's abyssal recipes) we have previously obtained ($\delta = \kappa/w$). But the previous scale did not have any information on the vertical velocity, which can now be obtained from the second and third scaling:

$$W = \frac{\beta U \delta}{f} \quad \text{and} \quad U = \frac{\Delta b \delta}{f L} \quad \text{gives} \quad W = \frac{\beta \delta^2 \Delta b}{f^2 L}. \quad (7.10)$$

This inserted into the scale for δ leads to a scale for the thickness

$$\delta = \left(\frac{\kappa f^2 L}{\beta \Delta b} \right)^{1/3} \quad (7.11)$$

and using the above to find a scale for W leads to

$$W = \left(\frac{\kappa^2 \beta \Delta b}{f^2 L} \right)^{1/3} \quad (7.12)$$

Some typical values for a subtropical gyre are

$$\begin{aligned} \Delta b &= 10^{-2} m s^{-2} \\ L &= 5000 km \\ f &= 10^{-4} s^{-1} \\ \kappa &= 10^{-5} m^2 s^{-2} \end{aligned}$$

and these values give us:

$$\delta = \left(\frac{10^{-5} \times 10^{-8} \times 5 \times 10^6}{10^{-11} 10^{-2}} \right)^{1/3} \approx 150 \text{ m} \quad (7.13)$$

$$W = \left(\frac{10^{-10} \times 10^{-11} \times 10^{-2}}{10^{-8} \times 5 \times 10^6} \right)^{1/3} \approx 10^{-7} \text{ m s}^{-1} \quad (7.14)$$

This vertical velocity is too small. The observed values of Ekman pumping velocities are on the order of 10^{-6} – 10^{-5} m s^{-1} . Using $\kappa = 10^{-5} \text{ m}^2 \text{ s}^{-2}$, which is too large!, would result in $\delta \approx 700 \text{ m}$ and $W \approx 4.6 \times 10^{-7} \text{ m s}^{-1}$.

The diffusive scaling is not sufficient and we will now build an adiabatic scaling estimate for the depth of the wind's influence.

An advective scale

Since the diffusive scaling is providing a vertical velocity much smaller than the Ekman pumping velocity at the top of the ocean, we conclude that we can ignore the diffusive term and the thermodynamic term completely, and construct an adiabatic scaling estimate for the depth of the wind's influence. Also, in subtropical gyres the Ekman pumping is downward, and the diffusive velocity is upward. This implies that at some level, D , we expect the vertical velocity to be zero.

The equation of motion are just thermal wind balance and linear geostrophic vorticity equation:

$$\beta v = f \frac{\partial w}{\partial z}, \quad f \frac{\partial \mathbf{u}}{\partial z} = \mathbf{k} \times \nabla b \quad (7.15)$$

and their scales are

$$\beta U = f \frac{W}{D}, \quad \frac{U}{D} = \frac{\Delta b}{fL}. \quad (7.16)$$

We take the vertical velocity to be that due to Ekman pumping, W_E . The depth scale of motion is thus

$$D = \left(\frac{W_E f^2 L}{\beta \Delta b} \right)^{1/2}. \quad (7.17)$$

If we relate U and W_E using mass conservation ($U/L = W_E/D$), instead of the Sverdrup balance, then

$$D = \left(\frac{W_E f L^2}{\Delta b} \right)^{1/2}. \quad (7.18)$$

The above estimate predicts a depth of the wind-influenced region (1) increasing with the magnitude of the wind stress (since $W_E \propto curl_z \tau$) and (2) decreasing with the meridional temperature gradient. The second dependency arises because a larger temperature gradient increases the thermal wind shear. Given that the horizontal transport (UD) is fixed by mass conservation, the only way that these two can remain consistent is for the vertical scale to decrease.

Taking $W_E = 10^{-6} \text{ m s}^{-1}$ or $W_E = 10^{-5} \text{ m s}^{-1}$, what would be the depth of the wind-influenced region D ? You will see that in both cases the estimate suggests that the wind-driven circulation is an upper ocean phenomenon ($\sim 500 \text{ m}$).

- The wind-influenced scaling D is the depth to which the directly wind-driven circulation can be expected to penetrate.
- Over the depth D we expect to see wind-driven gyres
- Below D lies the abyssal circulation, which is not wind-driven in the same way (but somehow it is ...)
- The thickness δ is the diffusive transition region between two different water masses: a warm subtropical water within the wind-driven layer and a cold dense water upwelling from the abyss.
- D is the depth of the thermocline. δ is the thickness of the thermocline (Fig. 7.4).

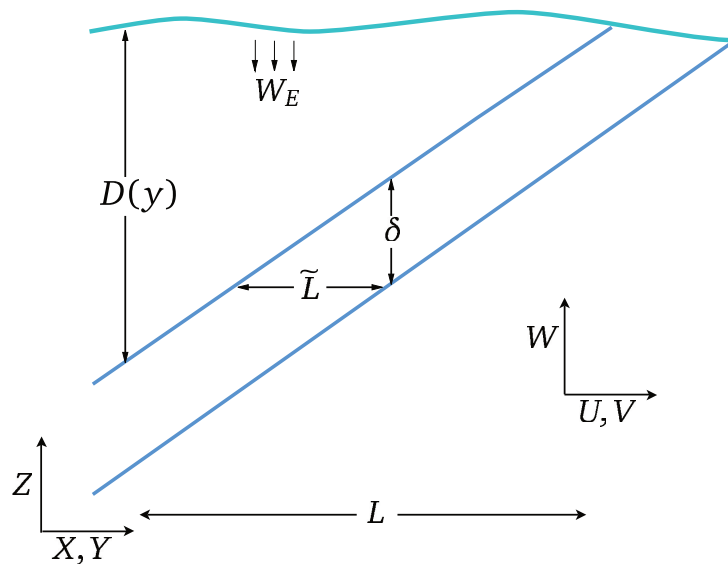


Figure 7.4: *Scaling of the thermocline. The diagonal lines mark the diffusive thermocline of thickness δ and depth $D(y)$. [from Vallis (2006)]*

7.2 A model for the oceanic abyssal flow: The Stommel-Arons model

In Munk's hypothesis, waters that fill the deep ocean can only return to the sea surface as a result of diapycnal eddy diffusion of buoyancy (heat and freshwater) downward from the sea surface. Munk's (1966) diapycnal eddy diffusivity estimate of $\kappa_v = 1 \times 10^{-4} \text{ m}^2 \text{ s}^{-1}$ was based on the idea of isolated sources of deep water and widespread diffusive upwelling of this deep water back to the surface. From all of the terms in the temperature and salt equations, Munk assumed that most of the ocean is dominated by the balance between vertical advection (upwards) and vertical diffusion (downwards; as in the diffusive thermocline):

$$w \frac{\partial T}{\partial z} = \kappa_v \frac{\partial^2 T}{\partial z^2}. \quad (7.19)$$

Munk obtained his diffusivity estimate of $10^{-4} \text{ m}^2 \text{ s}^{-1}$ from an average temperature profile and an estimate of about 1 cm/day for the upwelling velocity w , which can be based on deep-water formation rates and an assumption of upwelling over the whole ocean. But, the observed diapycnal eddy diffusivity in the open ocean away from boundaries is an order of magnitude smaller than Munk's estimate!. This means that there must be much larger diffusivity in some regions of the ocean – now thought to be at the boundaries, at large seamount and island chains, and possibly the equator. And, this also means that mechanical forcing must play a fundamental role in bringing large fraction of the water back to the surface.

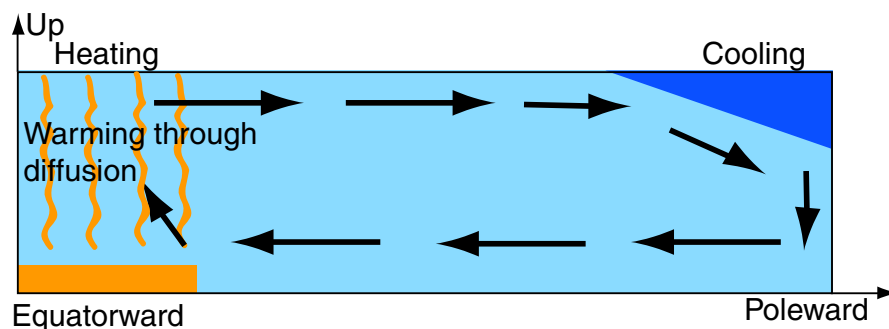


Figure 7.5: *The role of vertical (diapycnal) diffusion in the MOC, replacing a deep tropical warm source with diapycnal diffusion that reaches below the effect of high latitude cooling. [from Talley et al. (2011)]*

We will model the deep ocean as a single layer of homogeneous fluid in which there is a localized injection of mass at high latitudes (S_0), representing convection. Mass is extracted from this layer by upwelling into the warmer waters above it, keeping the average thickness of the abyssal layer constant. We assume that this upwelling is nearly uniform, that the ocean is flat-bottomed, and that a passive western boundary current may be invoked to satisfy mass conservation, and which does not affect the interior flow.

The planetary geostrophic momentum equations and mass continuity are

$$\mathbf{f} \times \mathbf{u} = -\nabla_z \phi \quad \nabla_z \cdot \mathbf{u} = 0. \quad (7.20)$$

Eliminating the pressure terms yields the vorticity balance

$$\beta v = f \frac{\partial w}{\partial z}. \quad (7.21)$$

The vertical velocity is positive and uniform at the top and zero at the bottom of the lower layer:

$$\beta v = f \frac{w_0}{H} \quad (7.22)$$

where w_0 is the uniform upwelling velocity and H is the layer thickness. The last equations tells us that, since by assumption $w_0 > 0$ (stretching of water columns), $v > 0$ and the flow is polewards everywhere and vanishing at the equator. The model is similar to the wind-driven circulation, but

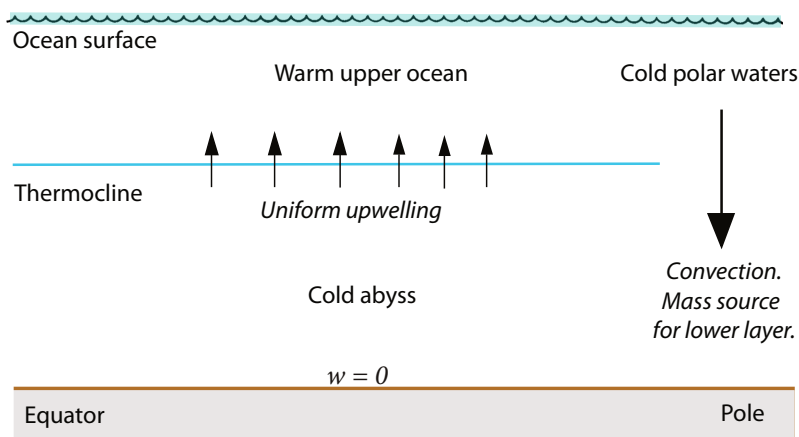


Figure 7.6: Stommel-Arons ocean model of the abyssal circulation. Convection at high latitudes provides a localized mass-source to the lower layer, and upwelling through the thermocline provides a more uniform mass sink. [from Vallis (2006)]

in the wind-driven case w_0 is the Ekman pumping. Here, it is the imposed uniform upwelling.

By geostrophic balance we have that

$$v = \frac{1}{f} \frac{\partial \phi}{\partial x} \quad (7.23)$$

so that the pressure is given by

$$\phi = - \int_x^{x_e} \left(\frac{f^2 w_0}{\beta H} \right) dx' = - \frac{f^2}{\beta H} w_0 (x_e - x) \quad (7.24)$$

assuming the boundary condition that $\phi = 0$ at $x = x_e$.

Using again geostrophic balance for the zonal velocity

$$u = - \frac{1}{f} \frac{\partial \phi}{\partial y} = \frac{1}{f} \frac{\partial}{\partial y} \left[\frac{f^2}{\beta H} w_0 (x_e - x) \right] = \frac{2}{H} w_0 (x_e - x). \quad (7.25)$$

Remembering that $\frac{\partial f}{\partial y} = \beta$ and $\frac{\partial \beta}{\partial y} = 0$.

This result is telling us that the zonal velocity is eastward, and independent of f and latitude y .

Are we conserving mass?

$$\frac{\partial u}{\partial x} + \frac{\partial v}{\partial y} + \frac{\partial w}{\partial z} = \frac{\partial}{\partial x} \left[\frac{2}{H} w_0 (x_e - x) \right] + \frac{\partial}{\partial y} \left[\frac{f w_0}{\beta H} \right] + \frac{w_0}{H} \quad (7.26)$$

$$= - \frac{2}{H} w_0 + \frac{w_0}{H} + \frac{w_0}{H} = 0 \quad (7.27)$$

7.2.1 A sector ocean

So far we have considered the effect of a uniform upwelling velocity, inducing a poleward flow. Let's now take a few steps toward a more realistic oceanic condition in which sources and sinks exist in the abyssal layer.

In our sector ocean, or rectangle in cartesian coordinates (Fig.7.12), we have a mass source at the northern boundary, balanced by uniform upwelling. Since the interior flow will be northwards, we anticipate a southwards flowing western boundary current to balance mass. Conservation of mass in the area polewards of a latitude y demands that

$$S_0 + T_I(y) - T_W(y) - U(y) = 0, \quad (7.28)$$

where S_0 is the strength of the source, T_W the equatorwards transport within the western boundary layer, T_I the polewards transport in the interior, and U is the integrated loss due to upwelling polewards of y .

Using Sverdrup balance, $v = (f/\beta)w_0/H$, the polewards transport through the section at latitude y is

$$T_I = \int_{x_W}^{x_E} vH dx = \int_{x_W}^{x_E} \frac{f}{\beta} w_0 dx = \frac{f}{\beta} w_0 (x_E - x_W). \quad (7.29)$$

The loss through upwelling is

$$U = \int_{x_W}^{x_E} \int_y^{y_N} w_0 dx dy = w_0 (x_E - x_W) (y_N - y). \quad (7.30)$$

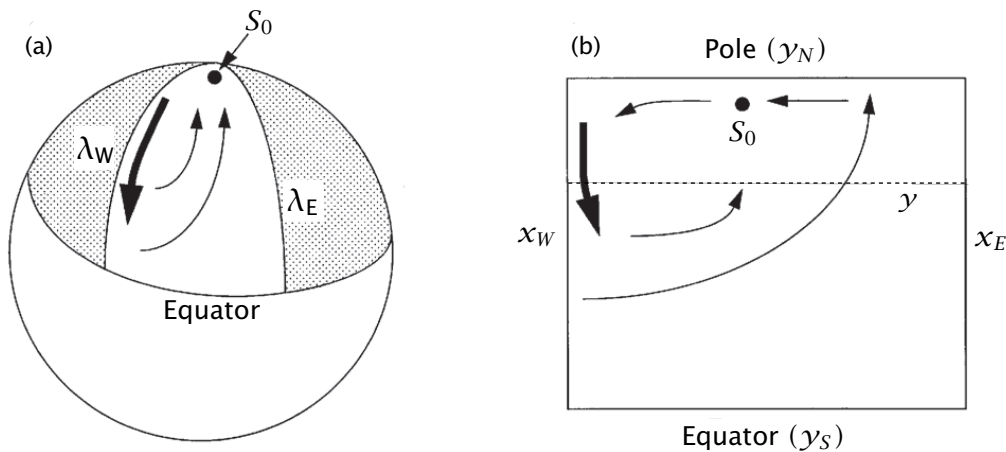


Figure 7.7: *Abyssal circulation in a spherical sector and in a corresponding Cartesian rectangle. [from Vallis (2006)]*

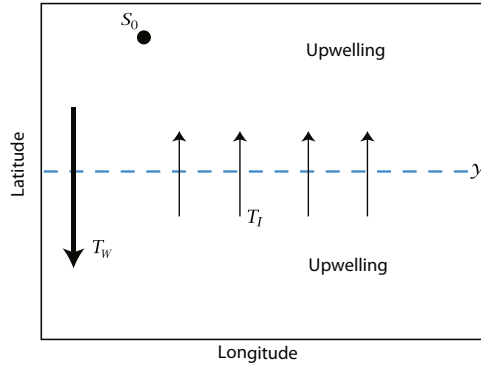


Figure 7.8: Mass budget in an idealized abyssal ocean. Polewards of some latitude y , the mass source (S_0) plus the poleward mass flux across y (T_I) are equal to the sum of the equatorward mass flux in the western boundary current (T_W) and the integrated loss due to upwelling (U) polewards of y . [from Vallis (2006)]

We can now estimate the strength of the western boundary current by using the two previous results:

$$T_W(y) = S_0 + T_I(y) - U(y) = S_0 + \frac{f}{\beta} w_0 (x_E - x_W) - w_0 (x_E - x_W) (y_N - y). \quad (7.31)$$

There is now a relationship we can use, ensuring mass balance over the entire basin, between sources S_0 and sinks U

$$S_0 = w_0 \Delta x \Delta y, \quad (7.32)$$

where $\Delta x = x_E - x_W$, and $\Delta y = y_N - y_S$.

$$T_W(y) = S_0 + \frac{f}{\beta} w_0 \Delta x - w_0 \Delta x (y_N - y) \quad (7.33)$$

$$T_W(y) = w_0 \Delta x (y_N - y_S) + \frac{f}{\beta} w_0 \Delta x - w_0 \Delta x (y_N - y) \quad (7.34)$$

$$T_W(y) = w_0 \Delta x \left(y - y_S + \frac{f}{\beta} \right). \quad (7.35)$$

Polewards of some latitude y , the mass source (S_0) plus the poleward mass flux across y (T_I) are equal to the sum of the equatorward mass flux in the western boundary current (T_W) and the integrated loss due to upwelling (U) polewards of y .

Given that y_S is our equator, we can set $y_S = 0$ and since $f = f_0 + \beta y$, we get

$$T_W(y) = w_0 \Delta x \left(2y + \frac{f_0}{\beta} \right). \quad (7.36)$$

Using mass balance $w_0 = \frac{S_0}{\Delta x y_N}$

$$T_W(y) = \frac{S_0}{y_N} \left(2y + \frac{f_0}{\beta} \right). \quad (7.37)$$

Now suppose the equatorial boundary of our domain is *at* the equator, which is what we have been thinking so far anyway, then $f_0 = 0$ and

$$\boxed{T_W(y) = 2S_0 \frac{y}{y_N}} \quad (7.38)$$

which at the northern boundary takes the form

$$T_W(y = y_N) = 2S_0. \quad (7.39)$$

A few conclusions so far

1. At the northern boundary the equatorward transport in the western boundary current is equal to twice the strength of the source!
2. The western boundary current is equatorwards everywhere.
3. The northward mass flux at the northern boundary ($f = \beta y_N$) is equal to the strength of the source itself, given that

$$T_I(y_N) = \frac{f}{\beta} w_0 \Delta x = \frac{f}{\beta} \frac{S_0}{y_N \Delta x} \Delta x = \frac{\beta y_N}{\beta} \frac{S_0}{y_N} = S_0. \quad (7.40)$$

The fact that convergence at the pole balances T_W and S_0 does not of course depend on the particular choice we made for f and y_S . The flow pattern evidently has the property of recirculation (see Fig.7.9 and Fig.7.10): this is one of the most important properties of the solution, and one that is likely to transcend all the limitations inherent in the model. This single-hemisphere model may be thought of as a crude model for aspects of the abyssal circulation in the North Atlantic, in which convection

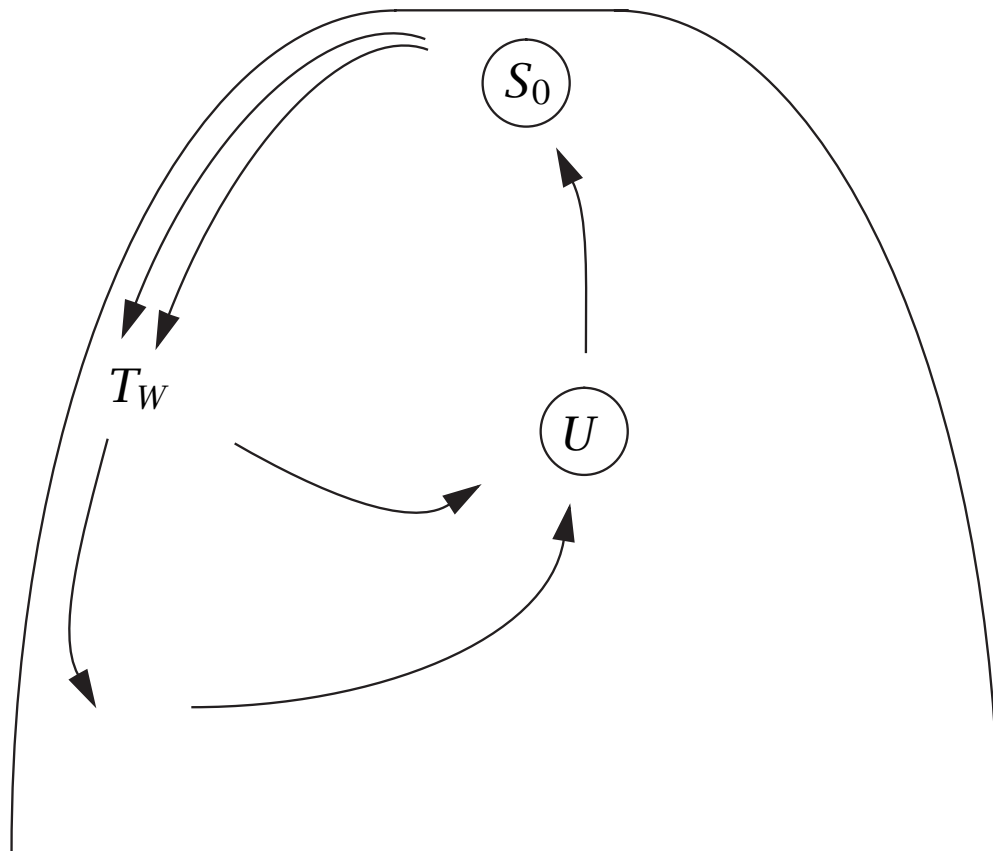
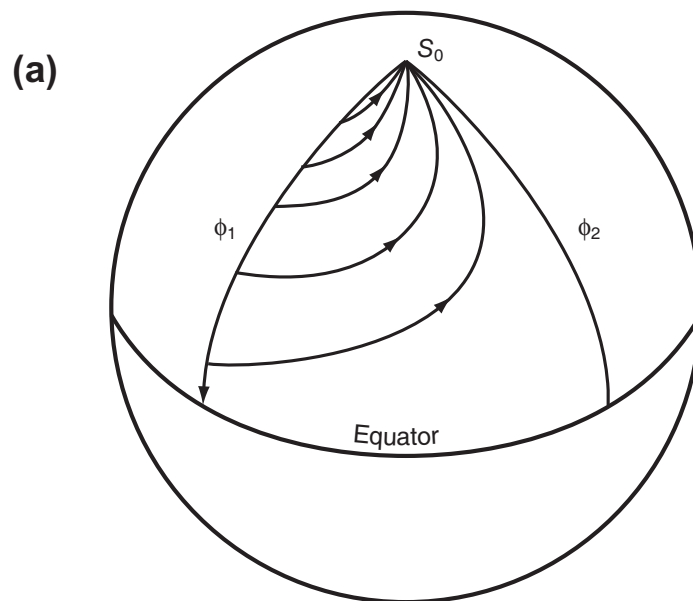


Figure 7.9: Schematic of a Stommel–Arons circulation in a single sector. The transport of the western boundary current is greater than that provided by the source at the apex, illustrating the property of recirculation. The transport in the western boundary current T_W decreases in intensity equatorwards, as it loses mass to the polewards interior flow, and thence to upwelling. The integrated sink, due to upwelling, U , exactly matches the strength of the source, S_0 . [from Vallis (2006)]

at high latitudes near Greenland is at least partially associated with the abyssal circulation.

The model can be expanded to a two-hemisphere basin, showing that a mass source in the Southern Hemisphere can drive deep recirculation in the opposite hemisphere. Later, a global map can be constructed with this simple model, qualitatively explaining deep circulation in the world oceans (Fig.7.11).

Perhaps the greatest success of the model is that it introduces the no-



(b)

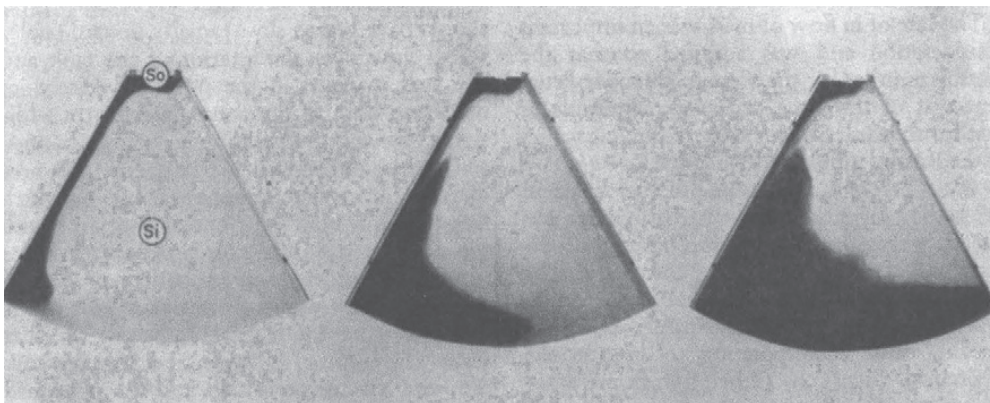


Figure 7.10: (a) *Abyssal circulation model. After Stommel and Arons (1960a).* (b) *Laboratory experiment results looking down from the top on a tank rotating counterclockwise around the apex (S_0) with a bottom that slopes towards the apex. There is a point source of water at S_0 . The dye release in subsequent photos shows the Deep Western Boundary Current, and flow in the interior S_I beginning to fill in and move towards S_0 . [from Talley et al. (2011)]*

tions of deep western boundary currents and recirculation – enduring concepts of the deep circulation that remain with us today. **This is a singular case in which a theoretical study predicted a major ocean current before it was actually observed!** For example, the North Atlantic ocean does

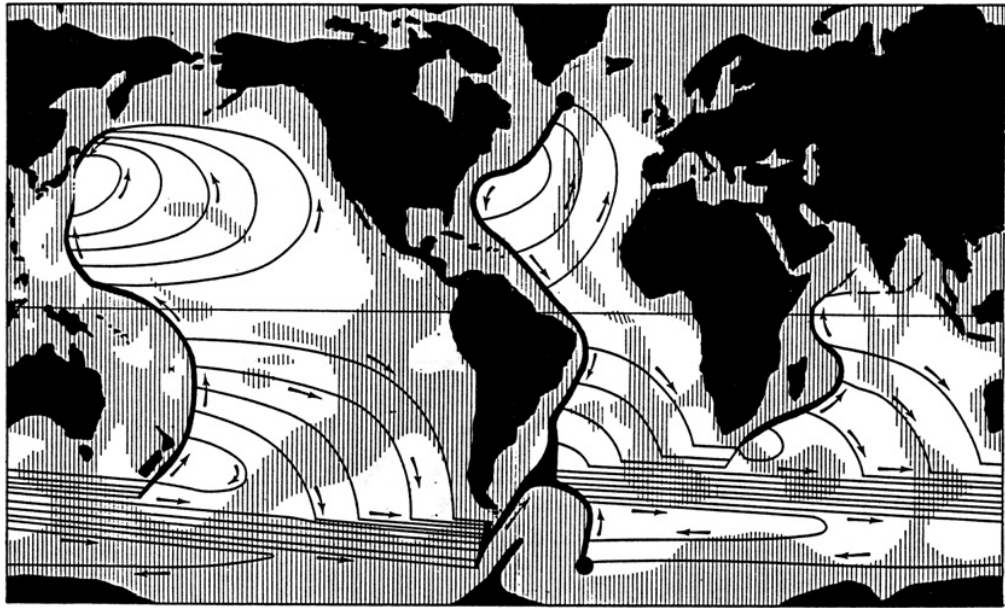


Figure 7.11: *Global abyssal circulation model, assuming two deep water sources (filled circles near Greenland and Antarctica). [from Talley et al. (2011)]*

have a well-defined deep western boundary current running south along the eastern seaboard of Canada and the United States. However, in other important aspects the model is found to be in error, in particular it is found that there is little upwelling through the main thermocline – much of the water formed by deep convection in the North Atlantic in fact upwells in the Southern Hemisphere.

An important assumption is that of uniform upwelling, across isopycnals, into the upper ocean, and that $w = 0$ at the ocean (flat) bottom. When combined with the linear geostrophic vorticity balance in the ocean abyss $\beta v = f \frac{\partial w}{\partial z}$, this gives rise to a poleward interior flow, and by mass conservation a deep western boundary current. The upwelling is a consequence of a finite diffusion, which in turn leads to deep convection as in the model of sideways convection. In reality, the deep water might not upwell across isopycnals at all, but might move along isopycnals that intersect the surface (or are connected to the surface by convection). If so, then in the presence of mechanical forcing a deep circulation could be maintained even in the absence of a diapycnal diffusivity. The circulation might then be qualitatively different from the Stommel–Arons model, although a linear vorticity balance might still hold, with deep western boundary currents.

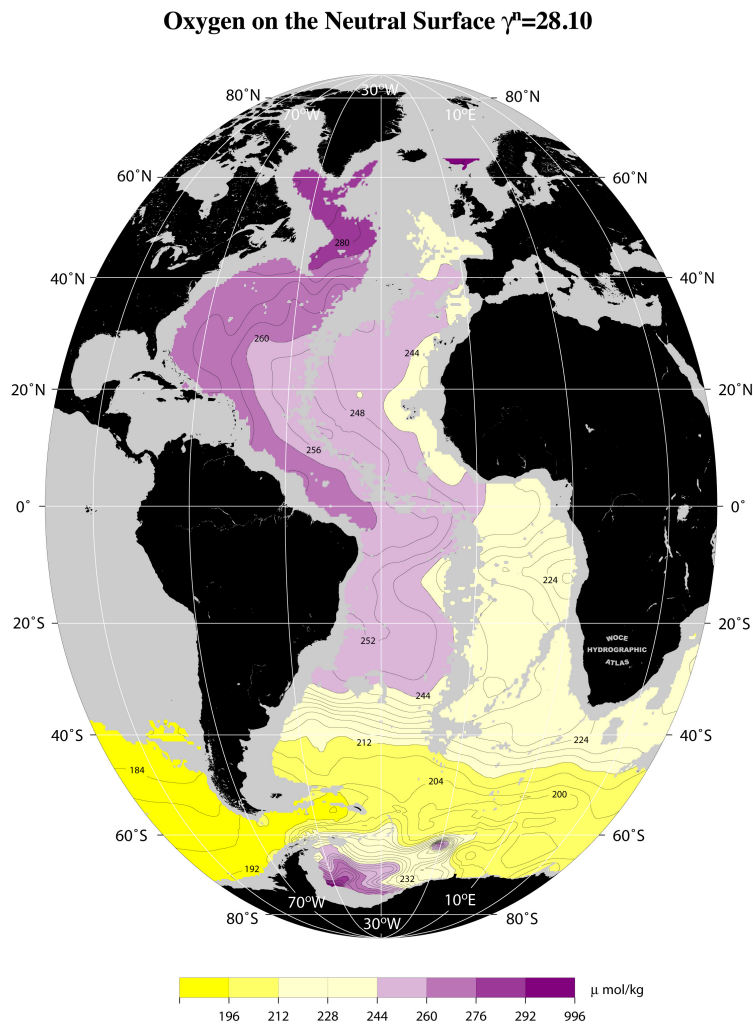


Figure 7.12: One feature of the solution is a deep western boundary current that flows southward in the Atlantic Ocean. This is consistent with observations. For example, high oxygen water is formed in the North Atlantic and flows southward in the deep western boundary current. [from the WOCE Atlas]

7.3 Wind-driven Overturning

Notes will be written soon. For now, please look at the slides shown in class.

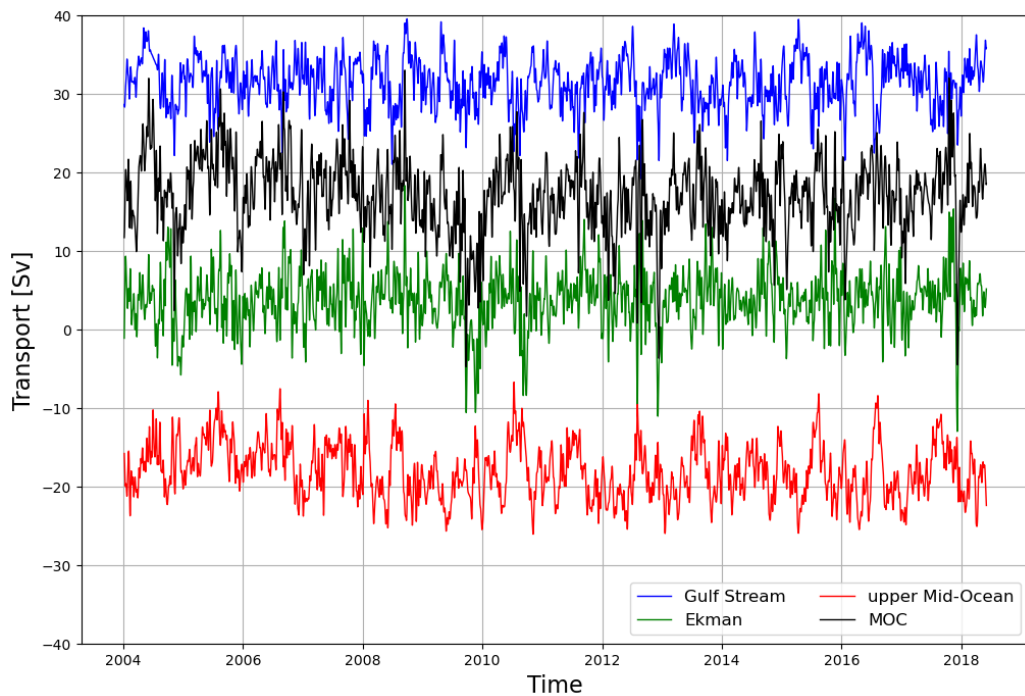


Figure 7.13: *Time series of different components of volume transports from the RAPID Array (2004-2019).*

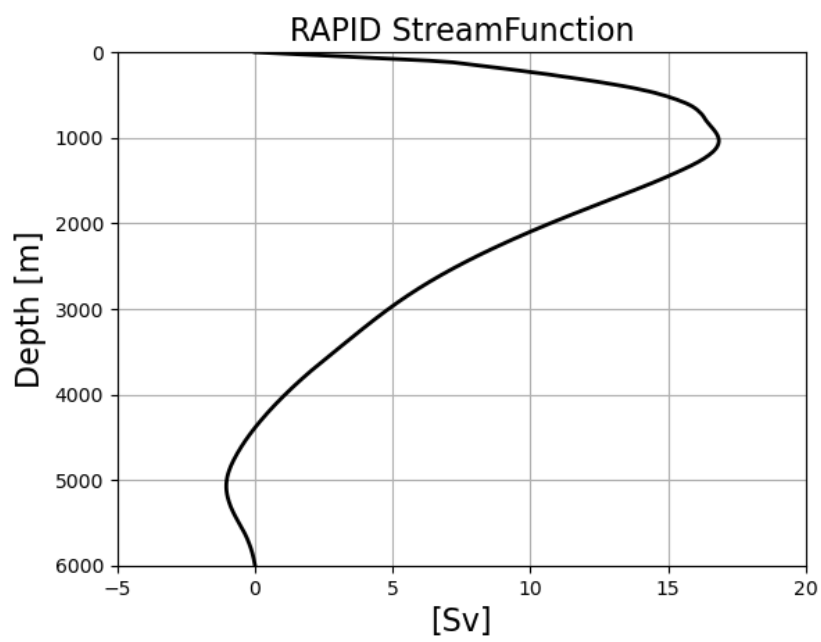


Figure 7.14: *Time mean (2004-2019) of the overturning stream function at 26.5N from RAPID.*

Bibliography

Talley, L., G. L. Pickard, W. J. Emery, and J. H. Swift, *Descriptive Physical Oceanography*, Academic Press, 560 pp, 2011.

Vallis, G. K., *Atmospheric and Oceanic Fluid Dynamics*, Cambridge Univ. Press, 745 pp, 2006.